

MINI-REVIEW



Experimental methods in chemical engineering: Thermogravimetric analysis—TGA

Nooshin Saadatkhah¹ | Adrián Carillo Garcia¹ | Sarah Ackermann² |
Philippe Leclerc¹ | Mohammad Latifi¹ | Said Samih¹ | Gregory S. Patience¹ |
Jamal Chaouki¹

¹Department of Chemical Engineering,
Polytechnique Montréal, Montréal,
Québec, Canada

²C-Therm Technologies, Thermal
Analysis Labs Division, Thermal Analysis
Labs Ltd., Fredericton, New Brunswick,
Canada

Correspondence

Jamal Chaouki, Department of Chemical
Engineering, Polytechnique Montréal,
C.P. 6079, Succ. CV Montréal, H3C 3A7
Québec, Canada.
Email: jamal.chaouki@polymtl.ca

Abstract

Thermogravimetric analysis (TGA) is a quantitative analytical technique that monitors the mass of a sample from 1 mg to several g as a furnace ramps temperature to as high as 1600°C under a stable or changing gas flow. The first gravimetric test was in 27 BC when Vitruvius measured limestone's change of mass as it calcined to lime. In modern chemical engineering, researchers apply the technique to derive conversions, kinetics, and mechanisms for any process with a change of mass by isothermal, non-isothermal, and quasi-isothermal methods. The mass drops as the sample decomposes, volatile compounds evaporate, or the oxidation state decreases, while in reactive environments (with O₂, for example), the mass of transition metals may increase. TGA is incapable of detecting phase transitions, polymorphic transformations, or reactions for which mass is invariant. DSC or DTA couple with TGA to help deconvolute a DSC plot by separating physical changes from chemical changes. Evolved gas analysis techniques monitor the gaseous products exiting the TGA furnace online as the temperature ramps. A bibliometric map of keywords from articles citing TGA indexed by *Web of Science* in 2016 and 2017 identified five research clusters: nanoparticles, performance, and films; crystal structures, acid, and oxidation; composites, nanocomposites, and mechanical properties; kinetics, pyrolysis, and temperature; and adsorption, water and wastewater, and aqueous solutions. This review provides an overview of the basic principles of modern TGA.

KEYWORDS

bibliometric map, kinetic analysis, material characterization, thermogravimetric analysis (TGA)

1 | INTRODUCTION

The International Confederation for Thermal Analysis and Calorimetry (ICTAC) defines thermal analysis (TA) as a group of techniques that monitor changes of physical or chemical properties of a sample with time as it is subjected to a temperature program. Thermogravimetric analyzers

(TGA) monitor and record sample mass, time, and temperature. The temperature program may include heating, cooling, isothermal holds, or a combination of them.^[1] The analyzer consists of a precise micro balance connected to a sample pan inside a furnace with a temperature programmer and controller—thermo-balance. The balance weighs the sample in a closed furnace.^[2]

We load the sample from the bottom (hang down), top, or side (Figures 1–3). A thermocouple near the pan monitors the sample temperature. A protective tube isolates both heating elements and cooling coils from the sample pan. A dynamic purge gas passes over the sample, at $20\text{--}200\text{ mL} \cdot \text{min}^{-1}$. The bottom-loading TGA supports the sample pan via a hang-down hook below the balance, and purge gas enters from a capillary tube from the side and exits on the opposite side of the pan (Figure 2).^[3] The top-loading TGA supports the sample pan and a thermocouple above the balance via a stem support rod. Purge gas typically enters from below the pan and exits from the top (Figure 1). In a side loading configuration, the sample

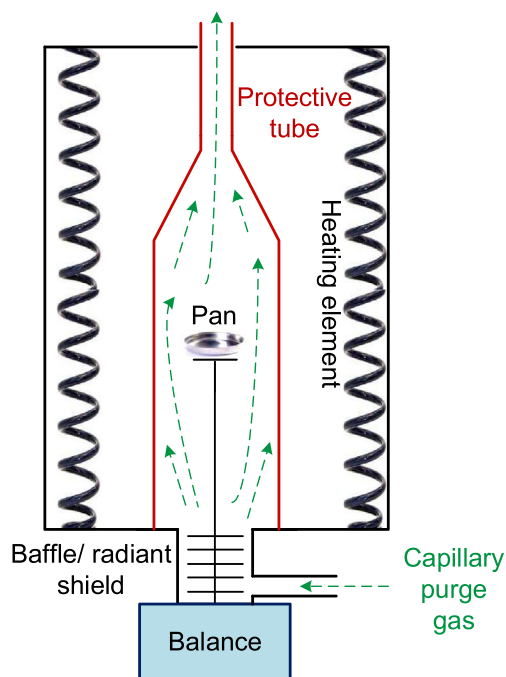


FIGURE 1 Top loading

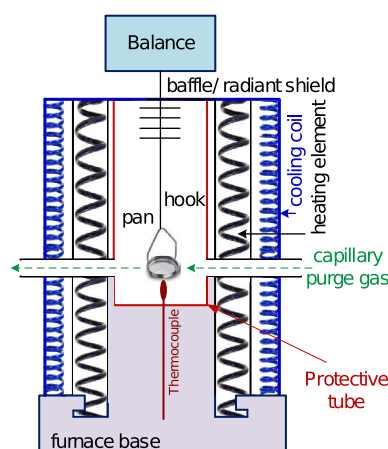


FIGURE 2 Bottom loading or hang down

support and furnace were orientated horizontally and purge gas flows over the surface of the pan (Figure 3).

The furnace, sample holder, gas entry, and exit points configuration minimizes the vigour of the turbulence near the sample pan and prevents noise in the mass flow signal. The heating elements and cooling coils are parallel to the flow stream in the top and side loading configurations.

A symmetrical electromagnetic balance has a counter pan as a counter-weight with small dynamic range. The counter pan serves to counteract the weight of the sample pan and the hangdowns or rods so that the sample mass changes are within the dynamic range of the balance (without the counterweight, a greater electromagnetic force is required to correct the effect of the hangdowns, sample pan, and sample crucible, which reduce balance sensitivity). Counter pans do not counteract buoyancy effects due to differences in gas flow rate and turbulence between the sample and counter pan. However, symmetrical TGAs are designed to counteract buoyancy effects. These TGAs use a high sensitivity symmetrical electromagnetic-optical balance, and instead of having the counter pan simply act as a counterweight, the counter pan is in its own furnace with a symmetrical gas flow arrangement (Figure 4). Two identical furnace chambers ensure that there is a symmetrical gas flow on both samples.

Capillary gases may be oxidizing, inert, or reducing. An oxidizing atmosphere, such as air or oxygen, combusts organic materials and oxidizes metals.^[4,5] Changing oxidation states complicates the analysis as the mass increases. An inert atmosphere, such as argon, helium, or nitrogen under low temperature conditions (when not studying metals such as Mg, which react with nitrogen) does not react with the sample. This enables studies of thermal stability and renders mass changes more readily attributable but yield higher residual carbons and on in the long term foul the instrument and exhaust gas lines. To minimize hazardous operating conditions, TGAs operate below the lower explosion limit (LEL) with dilute reactive capillary gases like hydrogen. Most TGAs operate

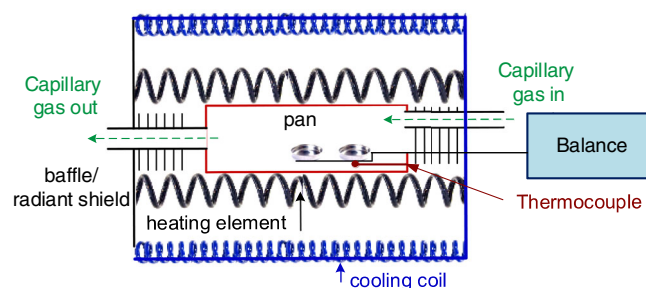


FIGURE 3 Side loading



FIGURE 4 Counter pan in its own furnace with a symmetrical gas flow arrangement

at ambient pressure; however, high pressure TGAs (HP-TGA) work up to 15 000 000 Pa and 1200°C.^[6]

In evolved gas analysis (TGA-EGA), gas chromatographs (GC), mass spectrometers (MS), Fourier transform infrared spectrometers (FTIR), or a combination of these, monitor the gaseous products on-line as the temperature ramps.^[7] TGA-FTIR is suited for water, carbon dioxide, SO_x, NO_x, HC, and common solvents, while for low effluent concentrations and complex mixtures, TGA-MS and TGA-GC/MS are necessary.^[8]

Differential scanning calorimetry (DSC) or differential thermal analysis (DTA) coupled with a TGA follows changes in heat flow and mass. This combination expands the capability of TGA alone as it detects changes due to reactions absent of mass loss or gain.^[9] TGA-DSC or TGA-DTA characterizes transitions like melting, crystallization, glass transition, and solid-solid transitions in addition to transformations with change of mass.

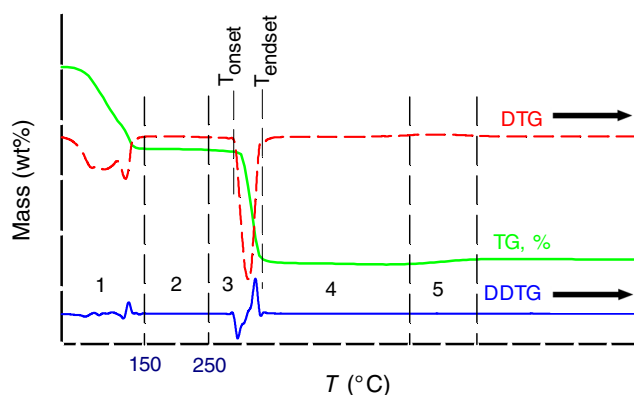


FIGURE 5 Five possible sections of a thermogram (TG curve (green), DTG curve, first derivative (red), DDTG curve, second derivative (blue) of $\text{Mn}(\text{CH}_3\text{CO}_2)_2 \cdot 4\text{H}_2\text{O}$ heated up to 900°C in air)

1.1 | Theory

A TG thermal curve or thermogram is a graphical representation of the sample mass change vs temperature or time. Thermograms are unique for each compound and communicate material thermal stability, oxidative stability, multi-component composition, product lifetime, decomposition kinetics, and moisture and volatile content. Generic thermograms have multiple sections (Figure 5)^[10,11]:

1. Below 150°C, physisorbed water, low molecular weight volatile compounds, solvents, and trapped gases evolve.
2. Between 150°C-250°C, mass loss is due to chemisorbed water and low molecular weight compounds like additives and volatile decomposition products.
3. Above 250°C, compounds begin to decompose between the onset and endset temperature. Multiple onset and endset temperatures are possible for multi-component systems and for reactions with intermediate steps.
4. The remaining material above the endset temperature includes non-volatile inorganic ashes and metals.
5. In an oxidizing environment, metallic compounds increase the oxidation state and gain mass.

The first and second derivatives of the weight loss profile (DTG and DDTG) identify inflection points and discriminate phenomena of multicomponent mixtures that react at overlapping temperatures (Figure 5).^[12–14] The peaks of the DTG correspond to inflection points, while for the case of overlapping peaks, the DDTG (onset temperatures) separate reactions more precisely.^[15] The temperature at which two extrapolated lines intersect is the onset temperature.

Physical properties that change as a function of time, t , are sources of kinetic data, and in thermogravimetry, the change in mass relates to the extent of conversion (α):

$$\alpha = \frac{W_0 - W(t)}{W_0 - W_\infty}, \quad (1)$$

where $W(t)$ is the mass of the sample at t ; and initial and residual masses are W_0 , W_∞ . α varies from 0-1. Distinct changes in the thermogram represent individual processes. The primary factors to identify these processes are temperature (T), pressure (P), and time (t)^[16]:

$$\frac{d\alpha}{dt} = k(T) f(\alpha) h(p). \quad (2)$$

Multi-step processes, like two parallel reactions, require more terms to fully characterize the system:

$$\frac{d\alpha}{dt} = k_1(T) f_1(\alpha) h_1(p) + k_2(T) f_2(\alpha) h_2(p), \quad (3)$$

where k is the linearized Arrhenius equation with respect to a reference temperature, T_0 :

$$k(T) = k_0 \exp\left(-\frac{E_a}{R} \left(\frac{1}{T} - \frac{1}{T_0}\right)\right), \quad (4)$$

where E_a is the activation energy; and k_0 is the reference kinetic rate constant at T_0 . Pressure affects the kinetics of reactions that produce gaseous compounds and reactions that depend on the partial pressure of the concentrations of gases introduced with the purge gas.

The reaction model in a variety of mathematical forms defines the α dependency. The power law,^[17] Avrami-Erofeev,^[18] contracting sphere, contracting cylinder, one-dimensional diffusion, two-dimensional diffusion reaction models, and three-dimensional diffusion (Jander or Ginstling-Brounshtein)^[19] are some of the common kinetic models in the solid-state (Table 1).^[20] For collecting kinetic data, maintain the moderate decomposition rate condition and set the purge gas flow at a rate that ensures the

immediate removal of the evolved gases. The immediate removal of gases prevents reverse reactions. The controlling factors are sample mass, gas atmosphere, and heating conditions, which are not independent of each other. Increasing the ramp rate or initial sample mass shifts the thermograms to higher temperatures (Figures 6 and 13).

1.2 | Description

Besides the temperature program, temperature ramp, hold-time, and maximum temperature, researchers select sample pans (aluminum, platinum, steel, copper, gold, glass, quartz, ceramic, or alumina), initial sample size, and gaseous environment (inert, oxidative, reductive, or reactive). Heat transfer and mass transfer rates from the purge gas to the sample are the highest with a shallow bed; however, precision is greater with a higher initial mass. Optimal sample volumes range from 50-500 μL . Platinum pans withstand temperatures up to 1000°C. However, ceramic pans are best for phosphorous samples as P reacts and degrades Pt under oxidative or inert atmosphere. A flame burns off most organic or polymer residues; therefore, for these applications, a Pt pan is suitable. For samples that form glassy residues that stick to the surface of the pans, inexpensive disposable Al pans are an acceptable choice. ASTM E1582, ASTM E2040, and ISO11358 describe the calibration of the weight scale and temperature of thermogravimetric analyzers. The ISO11358 is specifically devoted to the thermogravimetry (TG) of polymers.

2 | APPLICATIONS

In 2016 and 2017, over 11 300 articles indexed by WoS (*Web of Science*) mention thermogravimetric analysis.^[22] Most articles were in the category of polymer science

TABLE 1 Kinetic models used in the solid-state kinetics

No.	Reaction model	$f(\alpha)$
1	Power law ^[17]	$n\alpha^{(n-1)/n}$
2	One-dimensional diffusion	$\frac{1}{2}\alpha^{-1}$
3	Mampel (first order)	$1-\alpha$
4	Contracting sphere	$3(1-\alpha)^{\frac{2}{3}}$
5	Contracting cylinder	$2(1-\alpha)^{\frac{1}{2}}$
6	Two-dimensional diffusion	$[-\ln(1-\alpha)]^{-1}$
7	Avrami-Erofeev ^[18]	$n(1-\alpha)[- \ln(1-\alpha)]^{(n-1)/n}$
8	Three-dimensional diffusion ^[19]	$\frac{3}{2}(1-\alpha)^{\frac{2}{3}}[1-(1-\alpha)^{1/3}]^{-1}$

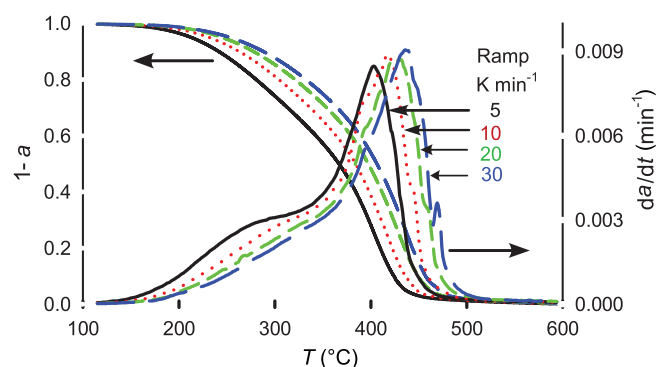


FIGURE 6 Bitumen mass loss as a function of temperature ramp. Increasing the ramp rate shifts the thermograms to higher temperatures^[21]

Of the top 10 000 cited articles, only 1153 were from chemical engineering journals and it was ranked in only 5 of the 112 categories that refer to the technique. VOSViewer software grouped keywords into five clusters based on bibliometric data (Figure 7).^[24] Nano particles, performance, films, carbon nanotubes, drug delivery, chitosan, fabrication, and surface are among the most frequently cited keywords in the red cluster with 34 of the top 110 keywords. The green cluster has the second highest number of keywords (26) and includes crystal structures, acid, oxidation, ionic liquids, complexes, MOF, coordination polymer, and metal organic framework. Composites, nanocomposites, mechanical properties, behaviour, polymers, degradation,

Of the top 10 000 cited articles in WoS, *RSC Advances* published 392, then appears *Journal of Applied Polymer Science* (307), *Journal of Thermal Analysis and Calorimetry* (235), *Bioresources* (112), *Polymer Composites* (110), *Energy & Fuels* (108), *Carbohydrate Polymers* (95), *Polymer Degradation and Stability* (87), *New Journal Of Chemistry* (84), and *Desalination and Water Treatment* (81).

As of March 2019, an article entitled “Characteristics of Hemicellulose, Cellulose and Lignin Pyrolysis” was cited 2352 times, which was more than any other article that

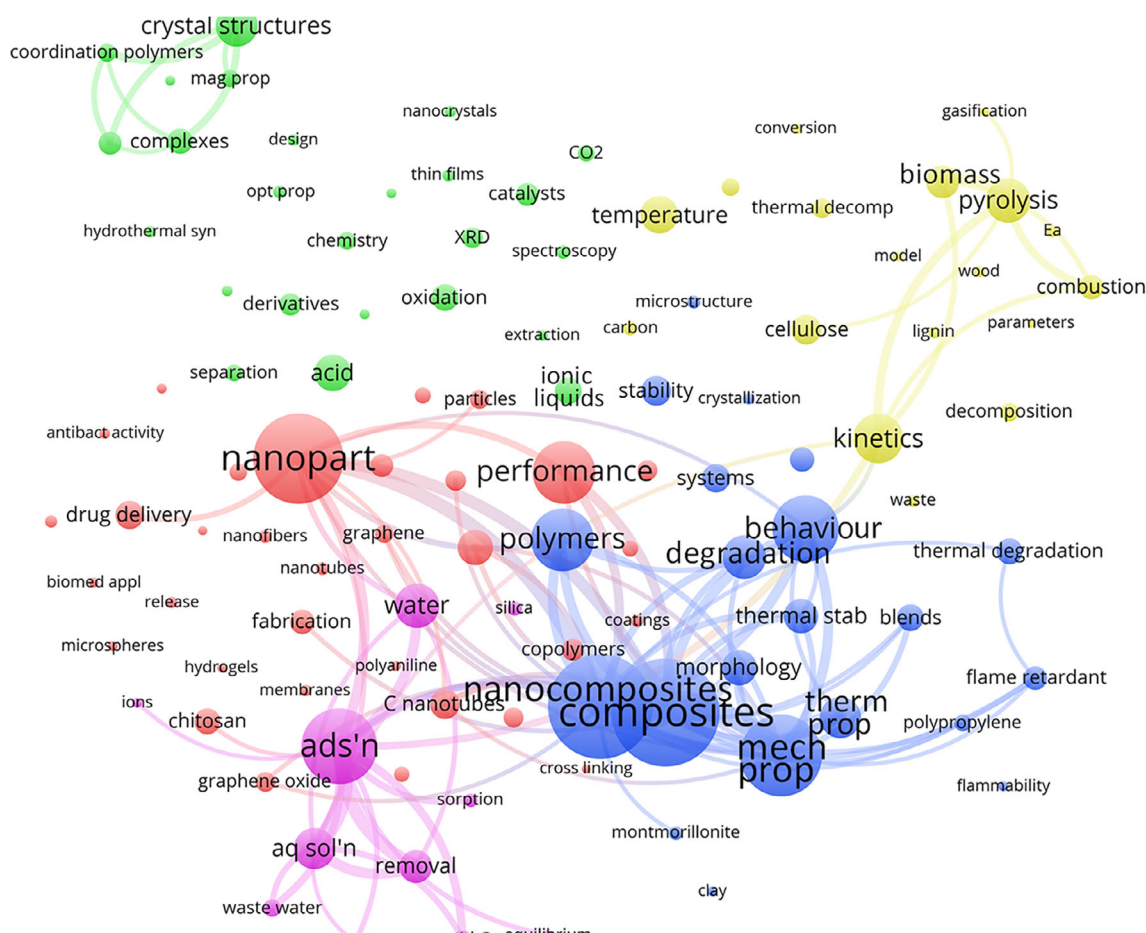


FIGURE 7 Thermogravimetric bibliometric map of 110 keywords from 10 000 of the most cited articles that WoS indexed in 2016 and 2017.^[24–26] The software assigns colours to keywords that are related and positions them in close proximity: nanoparticles (34 keywords), crystal structures (26), composites (20), kinetics (18), and adsorption (11). The size of the circle and font are proportional to the number of articles: nanoparticles (987 articles), crystal structures (458), composites (1174), kinetics (548), and adsorption (828). The smallest circles for each category are hydrogels (104), efficient (114), flammability (111), parameters (104), and equilibrium (108). The lines represent citation links

referred to thermogravimetric analysis.^[27] This work belongs mostly to the yellow cluster as it reviews the pyrolysis of biomass and includes lignin and cellulose among its keywords.

The keywords in the second and third most cited articles (“Alkanethiolate Gold Cluster Molecules with Core Diameters from 1.5 to 5.2 nm: Core and Monolayer Properties as a Function of Core Size” and “Chemical Oxidation of Multiwalled Carbon Nanotubes”)^[28] touch on the red cluster: nanoparticles and nanotubes.^[29] In the seven articles published by *The Canadian Journal of Chemical Engineering* in 2016 and 2017 researchers grafted poly(methyl methacrylate) from the surface of CNCs using aqueous, one-pot, free radical polymerization (yellow and blue clusters)^[30]; evaluated thermal behaviour of ground pine chip particles and ground pine pellet particles (yellow cluster)^[31]; synthesized NiFe_2O_4 spinel in solid state (green cluster)^[32]; tested the combustion characteristics and activation energy of the semi-char from an industrial circulating fluidized bed (yellow cluster)^[33]; monitored effects of NiO nanosorbants on adsorption and post-adsorption catalytic thermo-oxidative decomposition of vacuum residue asphaltenes (green and magenta clusters)^[34]; evaluated the fuel properties and the reaction characteristics of two different oil shales and sub-bituminous coal by non-isothermal thermogravimetric analysis (yellow and green cluster)^[35]; and analyzed the reaction model and dynamic reaction characteristics of limestone thermogravimetrically (yellow cluster).^[36]

3 | UNCERTAINTY

Conventional analyzers work with samples in the range of 5–50 mg: The uncertainty in all TGA systems depends most on the sensitivity of the balance. Another major source of error is related to sampling a heterogeneous powder: how does one select a representative sample from a batch that is several orders of magnitude larger in size.^[37] Withdrawing samples from bins and supersacks is problematic for TGA but also for particle size analysis, scanning electron microscopy, and most techniques that analyze or image particles. The golden rules of sampling advocates for withdrawing powder while it is in motion and taking it from the whole stream in short time increments rather than continuously taking a sample from part of the stream.^[38]

To test instrument precision, we completed three tests with 10 mg of polymethyl methacrylate powder (PMMA) ($d_p < 150 \mu\text{m}$) in a Q-5000 TA instrument at a heating rate of $10^\circ\text{C} \cdot \text{min}^{-1}$ with $40 \text{ mL} \cdot \text{min}^{-1}$ as the purge gas (Figure 8). The maximum difference in mass loss between the highest and lowest measurement reached 2.4% at 304°C , while the average difference was half that in the range of 280°C – 380°C . The average of the 95% confidence interval in this temperature range was 1.5°C .

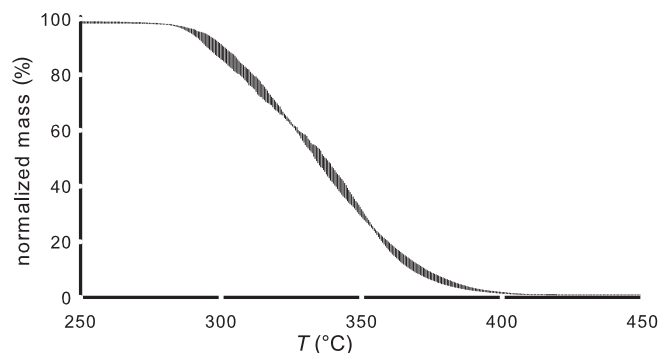


FIGURE 8 Mass loss of PMMA as a function of temperature. The plot shows the 95% confidence interval at 0.5°C intervals of three experiments with 10.4, 10.1, and 9.8 mg ($d_p < 150 \mu\text{m}$) at a heating rate of $10^\circ\text{C} \cdot \text{min}^{-1}$ and $40 \text{ mL} \cdot \text{min}^{-1}$ nitrogen

3.1 | Limitations

Limitations of conventional TGAs are related to sample size and heat and mass transfer rates. In samples with larger sizes, ($< 50 \text{ mg}$), heating rates within the sample are not rapid enough to ensure isothermal conditions, and poor mass transfer creates radial and axial concentration gradients.^[21,39–41] These limitations add uncertainty to kinetic parameters derived from conventional thermogravimetric analyzers (TGA).^[42]

Fluidized bed (FB-TGA),^[43] induction heating fluidized bed reactor (IHFB-TGA),^[44,45] and microwave (MW-TGA)^[46] thermogravimetric analyzers are emerging technologies that maximize heat transfer rates and, thus, minimize the limitations of conventional systems.

3.2 | Novel thermogravimetric analyzers

A FB-TGA comprises a quartz reactor, an electrical furnace, and sensing and controlling instruments: mass flow controllers, a load cell, thermocouples, and pressure transducers (Figure 9). The instrument maintains the bed at the minimum fluidization velocity at every temperature as the furnace heats the reactor. As much as 50 g of solid sample can be loaded into the FB-TGA, which operates at atmospheric pressure and temperatures from 25°C – 1200°C . Such a high mass of solids minimizes the uncertainty related to sampling. The 50 g loading of FB-TGA makes it suitable for a heterogeneous and complex feedstock like coal.^[43]

Operating an FB-TGA with hundreds of milligrams to a few grams maximizes mass transfer rates. However, an external heat source (tubular furnace, for example) ramps temperature up to $50^\circ\text{C} \cdot \text{min}^{-1}$, which generates a temperature gradient between the bed and crucible wall,

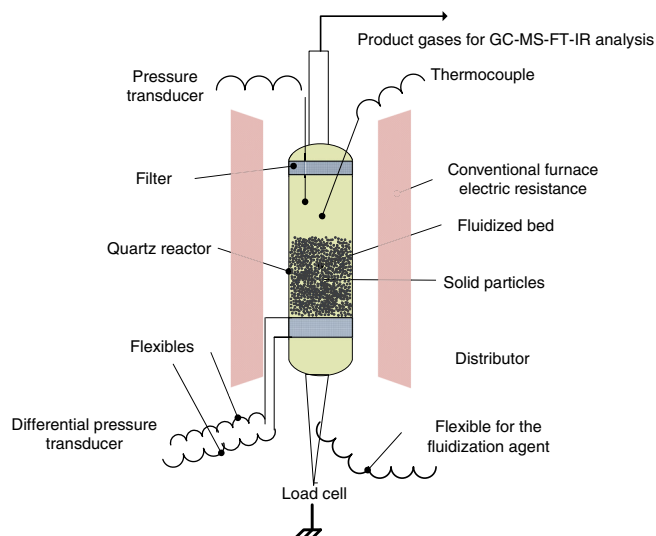


FIGURE 9 Schematic of a fluidized bed TGA^[43]

particularly for endothermic reactions. Gradients promote parasitic thermal reactions near the reactor wall; therefore, the overall reaction misrepresents the true process.^[42]

The IHFB-TGA overcomes heating rate limitations in micro reactors (as in FB-TGA) by induction heating. The IHFB has platinum rods 3 mm in diameter symmetrically placed in a circular configuration inside the reactor (Figure 10). A magnetic field created by a power supply induces an electric current with a high frequency (40 to 500 kHz); While convection and radiation transfer heat from the outside in, induction heating heats the bulk from the inside out. The IHFB-TGA is a perfect choice for developing processes that need a high heating rate such as the co-combustion of coal and waste.^[44]

The IHFB-TGA precisely controls temperature at heating rates up to $100^{\circ}\text{C} \cdot \text{s}^{-1}$. To maintain an isothermal bed a lift tube, hold the sample below the heated zone as the temperature increases. When the reaction zone reaches the set point, the lift tube rises up into the heated zone.

The MW-TGA, unlike conventional TGAs, pyrolyzes samples with microwaves. It includes an insulated quartz vessel (transparent to MW), an infrared thermopile, and a load cell (Figure 11). To heat non-polar samples, neutral microwave receptors like silicon carbide need to be added. Leclerc et al^[46] depolymerized polystyrene in a MW-TGA.

The limitations of FB-TGAs are related to working in the fluidized bed regime. Geldart group A and group B powders fluidize easily, while group C powders (cohesive) are difficult to work with. A narrow particle size range above $20 \mu\text{m}$ is best as the finer particles are carried up to the top of the vessel and block the filters. As a consequence, the pressure increases. Since the operating gas velocity is near minimum fluidization, solids mixing rates are low so a temperature gradient forms at the

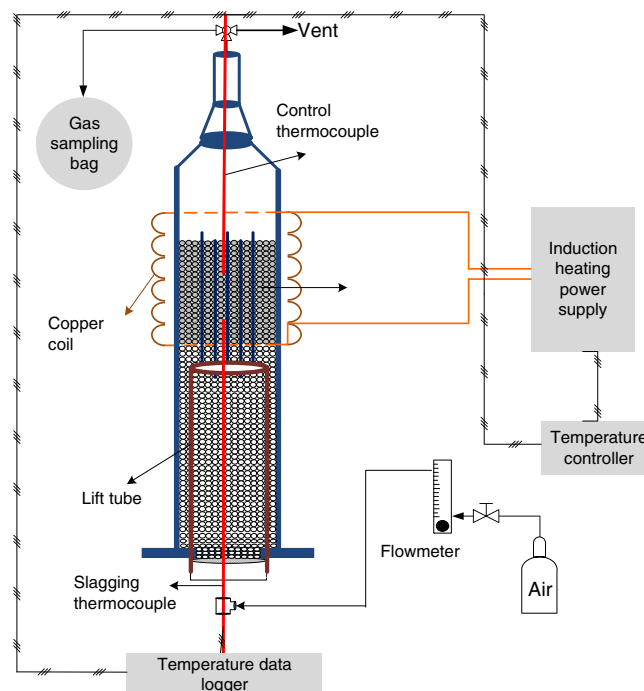


FIGURE 10 Schematic of an induction heating fluidized bed TGA apparatus^[44]

reactor wall (or in the vicinity of the SiC probe). The particle movement in the bed and at the grid induce fluctuations in the load cell that increases the uncertainty and noise in the mass measurement.

Noise or signal noise is an unwanted random addition to a wanted signal. A digital filter operates mathematical functions on a discrete time signal and reduces the noise signal, while an analog filter is an electronic circuit that operates on continuous analog signals. In Sigmaplot, regression or smoothing methods predict behaviour and estimate true values for a noisy dataset. Smoothing methods such as Loess and negative exponential smooth a TGA dataset either by removing undesired rapid variation and noises, or by resampling dependent variables to nearby independent variables. Labview has lowpass, highpass, bandpass, bandstop, or smoothing filters.

The IHFB-TGA contains metal parts, and unlike the FB-TGA, it measures the mass loss/gain based on on-line measurements of the outlet gases concentration by a multi-gas FTIR and/or a micro GC. Therefore, the outlet line should be at a high enough temperature to avoid the condensation of the gases before they enter the FTIR.

The limitations of a MW-TGA are related to the microwave powered working environment and to the non-intrusive temperature measurement (like pyrometers and infrared thermopiles). The microwave input power controls the heating rate; however, maintaining linear heating rates is problematic. The samples react in a microwave

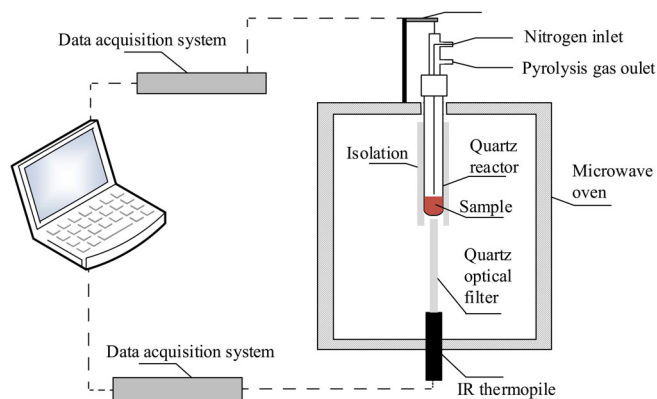


FIGURE 11 Schematic of microwave TGA apparatus^[46]

transparent vessel, but additional optical filters are required to measure the interior of the bed and not just the outer surface temperature.^[46] However, adding a optical filters limit the maximum temperature range of the instrument.^[46] The minimum reliable temperature measurement with a combination of silicon and quartz filters is 300°C. If the studied sample has a decomposition temperature below this temperature, the MW-TGA cannot detect it. Furthermore, an uncalibrated infrared thermopile induces error.

In a conventional TGA, sample mass and particle size must be small enough to avert external and internal heat and mass transfer diffusion resistances, making errors in derivation of kinetic parameters. While the minimum sample mass analyzed with a MW-TGA is 300 mg.^[46]

3.3 | Sources of error

The adequacy of the kinetic data derived from a TGA apparatus are related to either sample or instrument conditions, which change the controlling mass and heat transfer modes. The sample conditions involve sample form, sample size, and the sample holder (pan or crucible). Sample particle granularity controls the internal mass transfer resistance (Figure 12), while sample mass controls the external mass transfer resistance (Figure 13). The instrument conditions are temperature, the rate of temperature change, the gas atmosphere and its flow rate, and the pressure.

A thermocouple near the pan measures the furnace temperature and not the actual sample temperature. Thus, both the gas composition and flow rate influence what the temperature gauge reports. Vekemans et al.^[40] studied the temperature gradient between the thermocouple and the sample by developing a model in an infra-red furnace. The model assumed convection between the thermocouple and the sample holder was negligible and

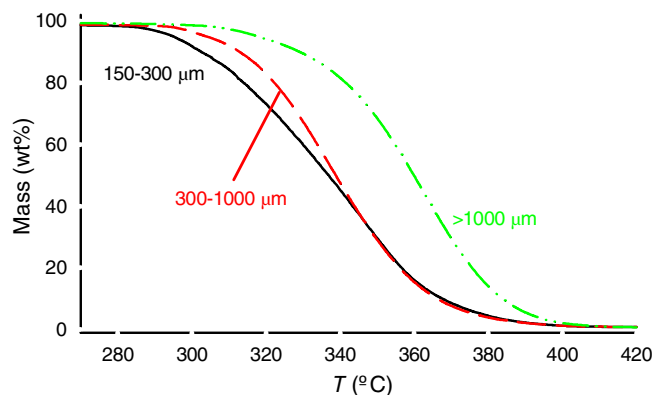


FIGURE 12 Effect of internal mass resistance on TGA. TG curves of a plastic sample with three different particle size distributions, $150 < d_p < 300 \mu\text{m}$, $300 < d_p < 1000 \mu\text{m}$, $1000 \mu\text{m} < d_p \mu\text{m}$ at a heating rate of $10^\circ\text{C} \cdot \text{min}^{-1}$ under $40 \text{ mL} \cdot \text{min}^{-1}$ nitrogen

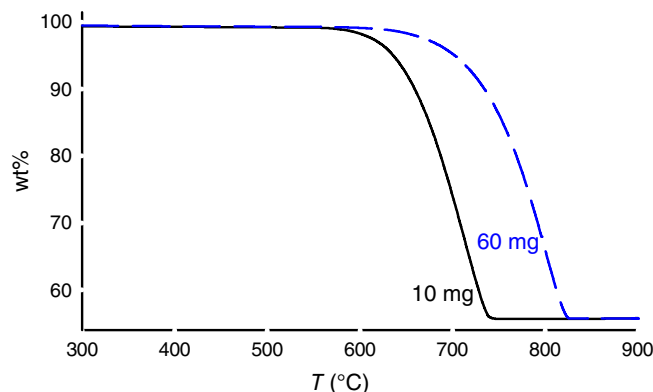


FIGURE 13 Effect of external mass transfer on TGA. TG curves of one calcite sample for 10 and 60 mg at a heating rate of $10^\circ\text{C} \cdot \text{min}^{-1}$ under $40 \text{ mL} \cdot \text{min}^{-1}$ nitrogen

the gas volume produced during the degradation was inconsequential compared to the inlet gas flow. Further, it ignored radiation and included only conduction and convection from the gas stream (Equation 5)^[40]:

$$F_{\text{gas}} C_{p,\text{gas}} (T_{\text{in}} - T_{\text{out}}) + US(T_F - T_S) = m C_{p,\text{sample}} \frac{dT_S}{dt} - \Delta H_{\text{rxn}} \frac{dm}{dt} \quad (5)$$

Another important factor that influences the true sample temperature in thermogravimetry is the effect of radiation on the sample temperature. Above 500°C, radiation becomes the dominant mechanism for heat transfer, especially when using an open-cup type sample pan; for example, a black sample can be at a temperature higher than a white sample at the same conditions.

Buoyancy is another phenomenon that decreases the accuracy either during heating or when switching between nitrogen and air, for example. As the temperature ramps, the gas density decreases, which translates to an apparent mass gain. This apparent mass gain depends on the volume of the pan and the density. Performing an experiment with an inert sample (empty pan) and subtracting this blank experiment can compensate for buoyancy and baseline issues.

4 | CONCLUSIONS

TGA characterizes physical and chemical changes of materials with temperature, by monitoring its change of mass. While the basic theory of a TGA seems really simple, it has many applications; it can be the first step to study many reactions, processes, and phenomena like heat and mass transfer.

Coupling TGA with DSC and gas phase analytical instruments like gas chromatography, mass spectrometry, and Fourier-transform infrared spectroscopy expands its capability to interpret complex overlapping phenomena. However, most TG analyzers resist up to 900°C, while some materials experience up to 1600°C during their production, service, and recycling like sintering of metal powders or incineration of industrial wastes. Researchers hope to improve thermogravimetric experiments by introducing new micro-TGA reactors like the FB-TGA, IHFB-TGA, and MW-TGA, which can mimic more industrial processes and reduce the limitations related to heat and mass transfer and operating temperature and pressure.

NOMENCLATURE

A	Arrhenius rate coefficient (s^{-1})
$C_{p, \text{ gas}}$	gas specific heat capacity ($J \cdot kg^{-1} \cdot K^{-1}$)
$C_{p, \text{ sample}}$	sample specific heat capacity ($J \cdot kg^{-1} \cdot K^{-1}$)
d_p	particle diameter (μm)
E_a	activation energy ($kJ \cdot kg^{-1}$)
F_{gas}	gas flow (inlet or outlet) ($kg \cdot s^{-1}$)
k	kinetic rate constant (s^{-1})
k_0	reference kinetic rate constant at T_0 (s^{-1})
m	mass of sample (kg)
P	pressure (Pa)
S	bottom surface area of the sample holder or pan (m^2)
T	Temperature (K)
T_{in}	inlet gas temperature (K)
T_{out}	outlet gas temperature (K)
T_F	thermocouple or furnace temperature (K)
T_S	sample temperature (K)

t	time (s)
U	global heat transfer coefficient ($W \cdot m^{-2} \cdot K^{-1}$)
$W(t)$	sample mass at t (g)
W_0	initial mass (g)
W_∞	residual mass (g)

Greek letters

α	extent of conversion varies from 0 to 1
ΔH_{rxn}	specific enthalpy of reaction ($J \cdot kg^{-1}$)

ACKNOWLEDGEMENTS

Brendan A. Patience collected the data from WoS and created the VoSViewer bibliographic map.

ORCID

Nooshin Saadatkhah  <https://orcid.org/0000-0002-3856-3197>

Gregory S. Patience  <https://orcid.org/0000-0001-6593-7986>

REFERENCES

- [1] S. Vyazovkin, A. K. Burnham, J. M. Criado, L. A. Pérez-Maqueda, C. Popescu, N. Sbirrazzuoli, *Thermochim. Acta* **2011**, 520, 1.
- [2] R. B. Prime, J. D. Menczel, H. E. Bair, S. Vyazovkin, P. K. Gallagher, A. Riga, in *Thermal Analysis of Polymers: Fundamentals and Applications* (Eds: J. D. Menczel, R. B. Prime), Wiley, Hoboken, NJ **2009**, p. 241.
- [3] M. E. Brown, *Introduction to Thermal Analysis: Techniques and Application*, Kluwer Academic Publishers, New York **2001**.
- [4] P. Tiwari, M. Deo, *AIChE J.* **2012**, 58, 505.
- [5] M. Edake, M. Dalil, M. J. D. Mahboub, J.-L. Dubois, G. S. Patience, *RSC Adv.* **2017**, 7, 3853.
- [6] L. Liu, Q. Liu, Y. Cao, W.-P. Pan, *J. Therm. Anal. Calorim.* **2015**, 120, 1877.
- [7] H. Paysepar, K. T. V. Rao, Z. Yuan, L. Nazari, H. Shui, C. C. Xu, *Fuel Process. Technol.* **2018**, 178, 362.
- [8] S. Singh, C. Wu, P. T. Williams, *J. Anal. Appl. Pyrol.* **2012**, 94, 99.
- [9] J.-P. Harvey, N. Saadatkhah, G. Dumont-Vandewinkel, S. Ackermann, G. S. Patience, *Can. J. Chem. Eng.* **2018**, 96, 2518.
- [10] M. J. D. Mahboub, J. Wright, D. C. Boffito, J.-L. Dubois, G. S. Patience, *Appl. Catal. A-Gen.* **2018**, 554, 105.
- [11] M. J. D. Mahboub, S. Lotfi, J.-L. Dubois, G. S. Patience, *Catal. Sci. Technol.* **2016**, 6, 6525.
- [12] S. A. El-Sayed, M. Mostafa, *Energ. Convers. Manage.* **2014**, 85, 165.
- [13] C. Saka, *J. Anal. Appl. Pyrol.* **2012**, 95, 21.
- [14] T. Fateh, F. Richard, T. Rogaume, P. Joseph, *J. Anal. Appl. Pyrol.* **2016**, 120, 423.
- [15] N. Saadatkhah, S. Aghamiri, M. R. Talaie, G. S. Patience, *Can. J. Chem. Eng.* **2018**, 97, 2299.

- [16] S. Vyazovkin, K. Chrissafis, M. L. Di Lorenzo, N. Koga, M. Pijolat, B. Roduit, N. Sbirrazzuoli, J. J. Suñol, *Thermochim. Acta* **2014**, 590, 1.
- [17] R. Ebrahimi-Kahrizsangi, M. Abbasi, *T. Nonferr. Metal. Soc.* **2008**, 8, 217.
- [18] T. Carvalho, P. Tavares, *Mater. Lett.* **2008**, 62, 3984.
- [19] J. Sun, Y. Huang, G. Gong, H. Cao, *Polym. Degrad. Stabil.* **2006**, 91, 339.
- [20] B. Janković, B. Adnadjević, J. Jovanović, *Thermochim. Acta* **2007**, 452, 106.
- [21] M. Cardona, D. C. Boffito, G. S. Patience, *Fuel* **2015**, 143, 253.
- [22] G. S. Patience, *Can. J. Chem. Eng.* **2018**, 96, 2312.
- [23] G. S. Patience, C. A. Patience, B. Blais, F. Bertrand, *Heliyon* **2017**, 3, e00300.
- [24] Clarivate Analytics, Web of Science Core Collection, <http://apps.webofknowledge.com> (accessed: June 2018).
- [25] N. J. van Eck, L. Waltman, *Scientometrics* **2010**, 84, 523.
- [26] G. S. Patience, C. A. Patience, F. Bertrand, *Can. J. Chem. Eng.* **2018**, 96, 811.
- [27] H. Yang, R. Yan, H. Chen, D. H. Lee, C. Zheng, *Fuel* **2007**, 86, 1781.
- [28] M. J. Hostetler, J. E. Wingate, C.-J. Zhong, J. E. Harris, R. W. Vachet, M. R. Clark, J. D. Londono, S. J. Green, J. J. Stokes, G. D. Wignall, G. L. Glish, M. D. Porter, N. D. Evans, R. W. Murray, *Langmuir* **1998**, 14, 17.
- [29] V. Datsyuk, M. Kalyva, K. Papagelis, J. Parthenios, D. Tasis, A. Siokou, I. Kallitsis, C. Galiotis, *Carbon* **2008**, 46, 833.
- [30] S. A. Kedzior, L. Graham, C. Moorlag, B. M. Dooley, E. D. Cranston, *Can. J. Chem. Eng.* **2016**, 94, 811.
- [31] H. Rezaei, F. Yazdanpanah, C. J. Lim, A. Lau, S. Sokhansanj, *Can. J. Chem. Eng.* **2016**, 94, 1863.
- [32] M. Chamoumi, N. Abatzoglou, *Can. J. Chem. Eng.* **2016**, 94, 1801.
- [33] Q. Ren, S. Bao, *Can. J. Chem. Eng.* **2016**, 94, 1676.
- [34] N. N. Marei, N. N. Nassar, M. Hmoudah, A. El-Qanni, G. Vitale, A. Hassan, *Can. J. Chem. Eng.* **2017**, 95, 1864.
- [35] D. K. Park, E. Song, *Can. J. Chem. Eng.* **2017**, 95, 2367.
- [36] M. Li, H. Yang, L. Song, Y. Wu, J. Liang, *Can. J. Chem. Eng.* **2017**, 95, 931.
- [37] J. A. Pazó, E. Granada, Á. Saavedra, P. Eguía, J. Collazo, *Int. J. Mol. Sci.* **2010**, 11, 3660.
- [38] T. Allen, *Particle Size Measurement*, 4th ed., Chapman and Hall, London **2012**.
- [39] O. Ebrahimpour, J. Chaouki, C. Dubois, *J. Mater. Sci.* **2013**, 48, 4396.
- [40] O. Vekemans, J.-P. Laviolette, J. Chaouki, *Thermochim. Acta* **2015**, 601, 54.
- [41] S. Samih, J. Chaouki, *Powder Technol.* **2017**, 316, 551.
- [42] S. Samih, M. Latifi, S. Farag, P. Leclerc, J. Chaouki, *Chem. Eng. Process.* **2018**, 131, 92.
- [43] S. Samih, J. Chaouki, *AIChE J.* **2015**, 61, 84.
- [44] M. Latifi, J. Chaouki, *AIChE J.* **2015**, 61, 1507.
- [45] M. Latifi, F. Berruti, C. Briens, *AIChE J.* **2014**, 60, 3107.
- [46] P. Leclerc, J. Doucet, J. Chaouki, *J. Anal. Appl. Pyrol.* **2018**, 130, 209.

How to cite this article: Saadatkhah N, Carillo Garcia A, Ackermann S, et al. Experimental methods in chemical engineering: Thermogravimetric analysis—TGA. *Can J Chem Eng.* 2020;98:34–43. <https://doi.org/10.1002/cjce.23673>